

# Rapid analysis of $^{13}\text{C}$ in plant-wax *n*-alkanes for reconstruction of terrestrial vegetation signals from aquatic sediments

**Kelsey E. McDuffee**

*Department of Earth System Science, University of California, 2222 Croul Hall, Irvine, California 92697, USA  
(kmcduffe@uci.edu)*

*Department of Marine Chemistry and Geochemistry, Woods Hole Oceanographic Institution, Woods Hole Road, MS 4, Woods Hole, Massachusetts 02543, USA*

**Timothy I. Eglinton**

*Department of Marine Chemistry and Geochemistry, Woods Hole Oceanographic Institution, Woods Hole Road, MS 4, Woods Hole, Massachusetts 02543, USA*

**Alex L. Sessions**

*Department of Geology and Geophysics, Woods Hole Oceanographic Institution, Woods Hole Road, MS 4, Woods Hole, Massachusetts 02543, USA*

*Division of Geological and Planetary Sciences, California Institute of Technology, Pasadena, California 91125, USA*

**Sean Sylva**

*Department of Geology and Geophysics, Woods Hole Oceanographic Institution, Woods Hole Road, MS 4, Woods Hole, Massachusetts 02543, USA*

**Thomas Wagner**

*Department of Geosciences, University of Bremen, Klagenfurter Strasse, P.O. Box 330440, D-28334 Bremen, Germany*

**John M. Hayes**

*Department of Geology and Geophysics, Woods Hole Oceanographic Institution, Woods Hole Road, MS 4, Woods Hole, Massachusetts 02543, USA*

[1] Long-chain, odd-carbon-numbered  $\text{C}_{25}$  to  $\text{C}_{35}$  *n*-alkanes are characteristic components of epicuticular waxes produced by terrestrial higher plants. They are delivered to aquatic systems via eolian and fluvial transport and are preserved in underlying sediments. The isotopic compositions of these products can serve as records of past vegetation. We have developed a rapid method for stable carbon isotopic analyses of total plant-wax *n*-alkanes using a novel, moving-wire system coupled to an isotope-ratio mass spectrometer (MW-irMS). The *n*-alkane fractions are prepared from sediment samples by (1) saponification and extraction with organic solvents, (2) chromatographic separation using silica gel, (3) isolation of straight-chain carbon skeletons using a zeolite molecular sieve, and (4) oxidation and removal of unsaturated hydrocarbons with  $\text{RuO}_4$ . Short-chain *n*-alkanes of nonvascular plant origin ( $<\text{C}_{25}$ ) are removed by evaporation on the moving wire. Test samples processed using this procedure yielded *n*-alkane fractions essentially free of interfering components. The  $\delta^{13}\text{C}$  values obtained by MW-irMS did not differ significantly from weighted averages of individual *n*-alkane  $\delta^{13}\text{C}$  values obtained by irmGC-MS. Isotopic variations in compound-class *n*-alkane fractions from a latitudinal transect of core-top sediments from the Southwest African margin ( $3^\circ\text{N}$ – $28^\circ\text{S}$ ) were congruent with those measured by compound-specific isotopic analyses of plant-wax *n*-alkanes. The amplitude of the variations was smaller, indicating contributions from non-plant-wax hydrocarbons, but the measurements revealed variations in carbon isotopic composition that are consistent with vegetation zones on the adjacent continent.

**Components:** 6200 words, 6 figures, 1 table.

**Keywords:** moving wire; plant-wax *n*-alkanes; stable carbon isotopes.

**Index Terms:** 4850 Oceanography: Biological and Chemical: Organic marine chemistry; 4894 Oceanography: Biological and Chemical: Instruments and techniques.

**Received** 10 June 2004; **Revised** 11 August 2004; **Accepted** 16 August 2004; **Published** 15 October 2004.

McDuffee, K. E., T. I. Eglinton, A. L. Sessions, S. Sylva, T. Wagner, and J. M. Hayes (2004), Rapid analysis of <sup>13</sup>C in plant-wax *n*-alkanes for reconstruction of terrestrial vegetation signals from aquatic sediments, *Geochem. Geophys. Geosyst.*, 5, Q10004, doi:10.1029/2004GC000772.

## 1. Introduction

[2] Photosynthesis in higher plants occurs through either the Calvin-Benson (C<sub>3</sub>) or the Hatch-Slack (C<sub>4</sub>) pathway. The carbon isotopic fractionations associated with these pathways differ significantly. Expressed in terms of δ<sup>13</sup>C (for simplicity and compactness, δ<sup>13</sup>C is herein abbreviated to δ) relative to Vienna Pee Dee Belemnite (VPDB), the carbon isotopic compositions of bulk tissues of C<sub>3</sub> plants commonly range from −25 to −30‰. C<sub>4</sub> plants are more enriched in <sup>13</sup>C, with −10 ≥ δ ≥ −16‰ for bulk tissue [Smith and Epstein, 1971; O'Leary, 1981; Collister et al., 1994]. The δ values of bulk organic carbon have been used to reconstruct the inputs of C<sub>3</sub> and C<sub>4</sub> plants from paleosols [Krishnamurthy and DeNiro, 1982; Guillet et al., 1988], lake sediments [Huang et al., 1999b], riverine suspended particulates [Mariotti et al., 1991], river sediments [Bird et al., 1994], and marine sediments [France-Lanord and Derry, 1994]. Oceanic sediments, however, commonly include both marine and terrigenous organic material, and both categories can include reworked fossil carbon [Wagner and Dupont, 1999]. Each of these components can have different isotopic compositions [Westerhausen et al., 1992; Meyers and Ishiwatari, 1993; Huang et al., 1999b]. To obtain a clearer view of inputs from higher plants, some means of focusing specifically on their products is required.

[3] Homologous series of *n*-alkanes, *n*-alcohols and *n*-alkanoic acids are abundant constituents of the epicuticular waxes found on leaves of terrestrial higher plants [Eglinton and Hamilton, 1963]. Plant-wax *n*-alkanes typically contain between 25 and 35 carbons, with a strong predominance of odd- over even-carbon-numbered chain lengths. This predominance is often expressed as the carbon preference index (CPI), where terrestrial higher plant waxes yield high values, usually greater than

4 [Collister et al., 1994]. Waxes on plant leaf surfaces are removed by rain and wind, especially by a sandblasting effect [Simoneit, 1977], and can then reach marine sediments through fluvial and eolian transport [Simoneit et al., 1977; Kawamura, 1995; Ohkouchi et al., 1997; Ikehara et al., 2000; Schefuß et al., 2003a, 2003b]. Measurement of the δ values of individual *n*-alkanes provides a signal related to terrestrial higher-plant-waxes and free of interference from other sources. This method has been successfully used to trace inputs from terrestrial vegetation into aerosols [e.g., Schefuß et al., 2003a] and aquatic sediments [e.g., Huang et al., 1999b, 2000; Freeman and Colarusso, 2001; Filley et al., 2001; Zhao et al., 2003; Schefuß et al., 2003b]. These and other studies demonstrate the potential of this approach to generate records with good fidelity and detail.

[4] The procedure is unfortunately complicated, time-consuming and expensive. Compound-specific isotopic analyses of individual *n*-alkanes can be obtained readily by isotope-ratio-monitoring GCMS (irmGCMS), but each analysis requires at least an hour and should be duplicated to minimize uncertainties. Recent advances in instrumentation offer a rapid method for measuring δ values by use of a moving-wire combustion system [Brand and Dobberstein, 1996] interfaced with an isotope-ratio mass spectrometer. Liquids are applied to the wire, which traverses in succession (1) a heated zone in which solvent is evaporated and (2) an enclosed, high-temperature furnace in which less-volatile components are combusted, with the CO<sub>2</sub> being transmitted to an isotope-ratio mass spectrometer. Using this system, aliquots of a plant-wax extract can be analyzed at 30 second intervals. With replicates, this provides complete isotopic analyses in less than 5 minutes.

[5] The rapidity with which measurements can be made using this approach offers the potential for

creating highly resolved isotopic records. In the present study, we developed and tested a procedure for the analysis of higher-plant-wax *n*-alkanes at the compound class level using moving-wire irMS. We address two questions: How successfully can high-throughput procedures isolate the desired analytes? How do the observed isotopic signals compare to those which could be obtained using irmGCMS? To examine these points, we have used both MW-irMS and irmGCMS to analyze surface sediments from the southwest African margin, an area well known for marked variations in inputs of vegetation from the adjacent continent.

## 2. Experimental

### 2.1. Reagents

[6] Solvents with ultra-low involatile residues, and thus with practically no contribution to the analytical blank, were obtained through subboiling distillation. Individual solvents (Fisher GC Resolv) were volatilized into nitrogen produced by evaporation of liquid nitrogen. Product was condensed at  $-13^{\circ}\text{C}$  (Thermo Neslab FTE 7) and collected in a pre-combusted glass flask. A single day of distillation produced 300–500 mL of clean solvent. Distilled solvents were stored at room temperature in pre-combusted glass bottles and used promptly. Rigorous removal of involatile organic residues from all solvents and reagents is crucial to the success of MW-irMS analyses.

### 2.2. Test Sediments

[7] Surface sediments from two sites (Table 1) were used to test the extraction and chemical isolation procedures. Sediments from Great Pond ( $41^{\circ}58.5'\text{N}$ ,  $70^{\circ}01.8'\text{W}$ ) were collected in July 1998 by raft with a hand-held Ekman dredge (0–10 cm depth). Great Pond is surrounded mainly by  $C_3$  vegetation, dominated by scrub oak (*Quercus* spp.) and pitch pine (*Pinus rigida*). Sediments from the “Mud Patch” ( $40^{\circ}30'\text{N}$ ,  $70^{\circ}45'\text{W}$ ) were collected by Mark III box core in April 1993 (2–5 cm depth). The latter site, a shallow depression on the New England shelf just south of Nantucket, is overlain by well-oxygenated bottom waters.

### 2.3. West African Sediments

[8] Core-top surface sediments (0–1 cm depth) were collected by multi-corer. Samples 4901-1 to 4918-4 were collected on *Meteor* cruise M34/2 between 29 January and 18 February, 1996 [Schulz and Scientific Party, 1996] and samples 3713-1 to

3701-1 were collected on *Meteor* cruise M41/2 between 13 February and 15 March, 1998 [Schulz and Scientific Party, 1998]. Bulk geochemical, bulk isotopic, and lignin data for these samples are presented by Wagner *et al.* [2004].

### 2.4. Extraction and Chemical Isolation of *n*-Alkanes

[9] The sediment purification scheme is outlined in Figure 1. Dried sediment samples (1 g) were saponified (0.5 M KOH in methanol, 10 mL) at  $70^{\circ}\text{C}$  for 2 hours in precombusted 40-mL vials. After cooling, Milli-Q  $\text{H}_2\text{O}$  was added (15 mL) and the neutral lipids were extracted with methyl tertiary-butyl ether (MTBE,  $3 \times 5$  mL). The aqueous layer of the saponified extract was subsequently adjusted to pH 1 with 4 N HCl, extracted with MTBE ( $3 \times 5$  mL) and archived. The neutral-lipid extract was then separated into four fractions using silica gel chromatography (0.5 g, 100–200 mesh, 5% deactivated), eluting with hexane (2.7 mL), dichloromethane (2.7 mL), ethyl acetate/dichloromethane (2/8, 5 mL), and methanol (2.7 mL), respectively. After evaporative concentration, the hydrocarbon fraction (F1) was placed on a zeolite molecular sieve column (Geokleen, GHGeochemical Services, 0.4 g, activated at  $450^{\circ}\text{C}$  for 4 hrs.) and eluted with hexane (4 mL) to remove branched and cyclic hydrocarbons. The zeolite column was dried overnight and the powder was transferred to a Teflon<sup>®</sup> vial. Concentrated hydrofluoric acid (48% HF) was added dropwise to dissolve the zeolite sieve. Samples were extracted with hexane ( $3 \times 1$  mL) and evaporated under a stream of  $\text{N}_2$ . Unsaturated and aromatic hydrocarbons were removed by oxidation with  $\text{RuO}_4$  (procedure modified from Huang *et al.* [1999a]).  $\text{RuO}_4$  was prepared by combining chloroform (6 mL),  $\text{NaIO}_4$  (2 g), Milli-Q  $\text{H}_2\text{O}$  (10 mL) and  $\text{RuO}_2 \cdot \text{H}_2\text{O}$  (10 mg) in a separatory funnel and shaking until a bright yellow color appeared, indicating formation of  $\text{RuO}_4$  in the organic phase. Drops of the  $\text{RuO}_4$  mixture were added to each sample and blown dry, repeating until the bright yellow color of the  $\text{RuO}_4$  persisted. Finally, samples were placed on a small (0.5 g, 100–200 mesh, 100% activated) silica gel column and eluted with hexane, yielding a clean *n*-alkane fraction.

### 2.5. Gas Chromatography (GC)

[10] Purified *n*-alkane fractions were analyzed on a Hewlett Packard (HP) 5890 II Plus GC fitted with a PTV inlet (Gerstel CIS-3), using a CP-Sil5-CB (Varian) column (60 m  $\times$  0.25 mm I.D., 0.25  $\mu\text{m}$

**Table 1.** Bulk Biogeochemical and Isotopic Data for All Sediment Samples

Site	Location	Water Depth, m	TOC, <sup>a</sup> %	C <sub>max</sub>	CPI <sup>b</sup>	ACL <sup>c</sup>	δ, ‰ (column heading indicates sample type)						
							mw	29	w1 <sup>d</sup>	w2 <sup>e</sup>	Δ(mw – w2)	Odd <sup>f</sup>	Even <sup>g</sup>
<i>Test Samples</i>													
Mud Patch (Marine, Massachusetts, USA)	40°30' N, 70°45' W	75	~1	29	2.97	28.77	-29.7	-30.1	-29.7	-29.7	0.0		
Great Pond (Truro, Massachusetts, USA)	41°58' N, 70°02' W	9	~20	27	4.62	27.99	-32.6	-32.4	-32.6	-32.5	-0.1		
<i>West African Samples</i>													
4901-1 <sup>h</sup>	2.68°N, 6.73°E	2177	0.81	29	2.69	28.85	-28.0	-29.2	-28.5	-28.5	0.5	-28.2	-29.4
4905-2	2.50°N, 9.39°E	1329	1.19	29	1.65	28.30	-29.0	-30.0	-29.4	-29.4	0.4	-29.5	-29.1
4906-4 <sup>h</sup>	0.69°S, 8.38°E	1272	1.51	29	2.32	29.00	-30.1	-33.3	-31.4	-31.4	1.3	-32.1	-30.5
4909-3	2.07°S, 8.63°E	1305	1.32	29	1.65	28.42	-29.3	-30.8	-29.7	-29.7	0.4	-30.0	-29.4
4912-3 <sup>h</sup>	3.73°S, 9.79°E	1298	1.49	29	1.73	28.69	-29.5	-33.5	-32.9	-32.9	3.4	-33.0	-32.8
4913-4 <sup>h</sup>	5.50°S, 11.07°E	1300	1.65	29	2.12	28.63	-29.5	-31.2	-29.9	-29.9	0.4	-30.4	-29.4
4915-3 <sup>h</sup>	7.75°S, 11.87°E	1305	1.33	29	1.37	28.53	-28.7	-30.2	-29.4	-29.4	0.7	-29.7	-29.2
4916-3	10.17°S, 12.69°E	1300	2.53	29	2.03	28.20	-28.5	-30.1	-29.4	-29.4	0.9	-29.5	-29.3
4917-5	11.91°S, 13.07°E	1299	2.16	29	1.71	28.60	-28.8	-29.7	-29.1	-29.1	0.3	-29.1	-29.1
4918-4	12.84°S, 12.70°E	1338	2.21	29	1.93	28.71	-28.5	-29.0	-28.5	-28.5	0.0	-28.1	-29.0
3713-1 <sup>h</sup>	15.63°S, 11.58°E	1330	1.17	31	2.29	29.22	-27.9	-29.4	-28.3	-28.3	0.3	-28.0	-28.9
3712-1	17.19°S, 11.13°E	1242	1.62	31	2.09	28.54	-27.9	-27.8	-28.4	-28.4	0.4	-27.9	-28.8
3715-3 <sup>h</sup>	18.96°S, 11.06°E	1350	3.37	31	2.55	29.22	-28.3	-27.9	-27.9	-27.8	-0.5	-27.2	-29.2
3711-1	19.84°S, 10.77°E	1214	2.71	31	2.35	28.60	-27.5	-28.8	-28.9	-28.9	1.4	-28.3	-29.9
3710-1	20.66°S, 11.40°E	1313	3.53	27	1.29	28.32	-27.9	-29.0	-29.0	-29.0	1.1	-28.9	-29.0
3708-1	21.09°S, 11.83°E	1283	3.25	29	1.51	28.70	-28.4	-28.7	-28.8	-28.8	0.4	-28.3	-29.2
3707-3 <sup>h</sup>	21.63°S, 12.19°E	1350	3.37	29	2.39	29.20	-28.2	-28.1	-28.1	-28.0	-0.2	-27.3	-29.2
3706-3	22.72°S, 12.60°E	1313	2.94	29	1.54	28.70	-28.3	-28.9	-28.8	-28.8	0.5	-28.1	-29.5
3718-4 <sup>h</sup>	24.90°S, 13.16°E	1316	4.12	31	2.20	29.24	-28.0	-28.4	-28.1	-28.1	0.0	-27.3	-29.5
3703-4	25.52°S, 13.23°E	1376	6.07	31	2.37	28.87	-27.0	-28.7	-28.4	-28.4	1.3	-27.8	-29.2
3702-2 <sup>h</sup>	26.79°S, 13.46°E	1319	3.09	31	1.93	29.14	-28.5	-28.9	-28.4	-28.4	-0.2	-27.7	-29.4
3701-1 <sup>h</sup>	27.95°S, 14.00°E	1488	1.09	31	1.60	28.97	-28.8	-29.4	-28.8	-28.7	0.0	-28.2	-29.5

<sup>a</sup> Wagner et al. [2003].

<sup>b</sup> CPI = 0.5\*Σ(X<sub>27</sub> – X<sub>33</sub>)/(X<sub>26</sub> – X<sub>32</sub>) + 0.5\*Σ(X<sub>27</sub> – X<sub>33</sub>)/(X<sub>28</sub> – X<sub>34</sub>), where X is abundance.

<sup>c</sup> Average chain length = Σ(i\*X<sub>i</sub>)/Σ X<sub>i</sub>, where X is abundance and i = C<sub>25</sub> – C<sub>33</sub>.

<sup>d</sup> δ<sub>w1</sub> = Σ X<sub>i</sub>\*δ<sub>i</sub>, where X is the fraction of total *n*-alkane abundance and δ is the individual *n*-alkane δ value determined by irmGC-MS, with i = 21 to 34, or for all *n*-alkanes with individual δ values.

<sup>e</sup> δ<sub>w2</sub> = Σ X<sub>i</sub>\*δ<sub>i</sub>, where X is the fraction of the total *n*-alkane abundance assuming evaporation of *n*-alkanes equivalent to that at 90C off the moving wire (Figure 3a) and δ is the individual *n*-alkane δ value determined by irmGC-MS, with i = 21 to 34, or for all *n*-alkanes with individual δ values.

<sup>f</sup> δ<sub>odd</sub> = Σ X<sub>i</sub>\*δ<sub>i</sub>, where X is the fraction of total *n*-alkane abundance including evaporation and δ is the individual *n*-alkane δ value determined by irmGC-MS, with i = 27 to 33, for all odd numbered *n*-alkanes.

<sup>g</sup> δ<sub>even</sub> = Σ X<sub>i</sub>\*δ<sub>i</sub>, where X is the fraction of total *n*-alkane abundance including evaporation and δ is the individual *n*-alkane δ value determined by irmGC-MS, with i = 26 to 32, for all even numbered *n*-alkanes.

<sup>h</sup> Contribution of *n*-C<sub>34</sub> calculated as 0.3\**n*-C<sub>32</sub>, based of ratio of C<sub>34</sub>/C<sub>32</sub> in unfootnoted samples.

film thickness). The column temperature was held at 40°C for 1 min, programmed to 120°C at 30°/min and then to 320°C at 6°/min, and finally held at 320°C for 18 min. Helium (constant flow, 2 mL/min) was used as the carrier gas.

## 2.6. Compound-Specific Carbon Isotopic Analyses (irmGCMS)

[11] A Hewlett Packard 6890 GC interfaced to a modified Finnigan GC Combustion III unit and a

Finnigan Delta<sup>Plus</sup> isotope ratio mass spectrometer was used for compound-specific isotopic analyses. Compounds were separated on a Factor Four VF-1ms capillary column (60 m × 0.32 mm I.D., 0.25 μm film thickness). The column temperature was held at 60°C for 3 min, programmed to 150°C at 60°/min and then to 340°C at 8°/min, and finally held at 340°C for 13.5 minutes. During each analysis, pulses of reference CO<sub>2</sub> were admitted to the mass spec-



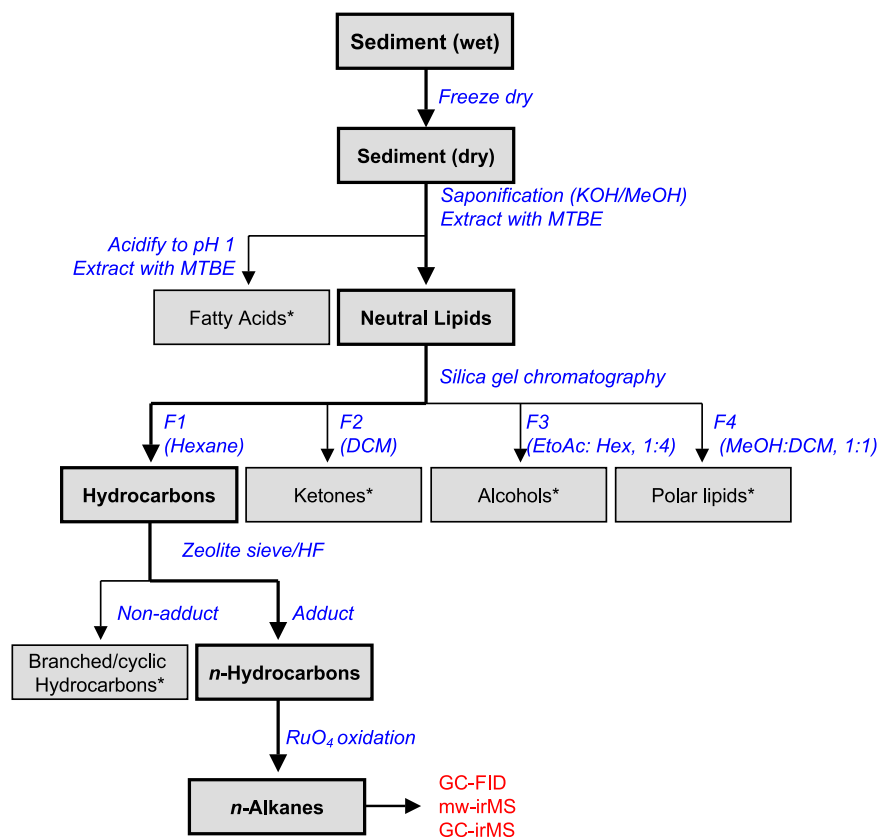


Figure 1. Chemical isolation and purification scheme.

trometer and were used for calibration relative to the VPDB standard.

## 2.7. Compound-Class Carbon Isotopic Analyses by Moving-Wire irMS (MW-irMS)

[12] The moving-wire combustion system [Brand and Dobberstein, 1996] (Figure 2) consists of a low-carbon Ni wire (0.25 mm diameter) pulled through a series of heating and coating stages at the rate of 2 cm/sec. After leaving the supply spool, the wire passes through a 900°C cleaning oven which serves both to remove any organic contamination and to oxidize the surface of the wire. The sample (100–200 ng C) is then added to the wire either by HPLC or as a single 1- $\mu$ L droplet from a standard syringe. The wire continues over a drying element whose temperature can be adjusted from 30 to 200°C. The solvent is evaporated by convecting warm air, leaving the nonvolatile sample on the wire. The wire continues into a furnace (800°C), where organic material on the wire is combusted. The furnace is purged by 25 mL/min He. Oxygen for combus-

tion is derived from NiO on the surface of the wire and from CuO inside the combustion furnace. The latter is regenerated daily by exposure to pure O<sub>2</sub>. The effluent from the combustion furnace (25 mL/min less the flows that escape around the wire at the end fittings of the combustion reactor) then passes through a Nafion-membrane drier to remove water. An open split directs 0.2 mL/min to a Finnigan-MAT 252 isotope ratio mass spectrometer. Drops are applied to the wire every 30 seconds. External standards (cholestanol and glucose) are analyzed after every fifth sample and CO<sub>2</sub> pulses are inserted at the beginning and end of each run and between samples.

[13] Reported  $\delta$  values are means of five measurements. The pooled standard deviation for the population of single observations of glucose and cholestanol standards is 0.27‰ (77 degrees of freedom, where degrees of freedom = number of analyses ( $n$ ) – number of sets of replicates ( $m$ ); here  $n = 96$  and  $m = 19$ ). Similarly, the pooled standard deviation for the population of single observations of *n*-alkane fractions is 0.27‰

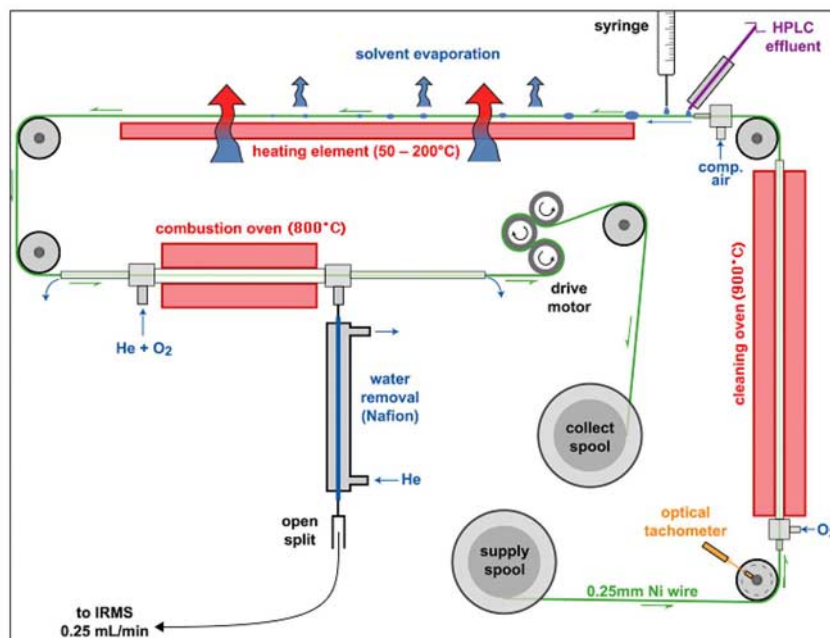


Figure 2. Schematic diagram of moving-wire system.

(132 degrees of freedom, where  $n = 166$  and  $m = 34$ ). The 95% confidence interval for the mean of five replicates is then  $\pm 2[(0.27)/(\sqrt{5})] = \pm 0.24\%$ .

### 3. Results and Discussion

#### 3.1. Optimization of Conditions for MW-irMS

[14] Marine sediments potentially contain *n*-alkanes derived from terrestrial plant waxes, marine production, and petroleum or other fossil sources. Marine and petroleum sources usually consist of lower molecular weight *n*-alkanes. The terrestrial higher-plant-wax signal, typically at  $C_{25}$  and higher, was therefore selected by evaporating the shorter chain *n*-alkanes from the moving wire prior to combustion. To test the effectiveness and potential isotopic fractionations associated with this approach, eleven *n*-alkane standards ( $C_{18}$ – $C_{26}$ ,  $C_{28}$ ,  $C_{30}$ ) were analyzed by MW-irMS at different drying-oven temperatures.

[15] *n*-Alkane standards were applied to the moving wire in hexane (boiling point  $68.7^\circ\text{C}$ ). At the wire speeds used in this work, even at room temperature, a  $1\text{-}\mu\text{L}$  drop of hexane evaporated completely before the wire reached the combustion reactor. The extent of evaporation of larger alkanes

was determined by measuring yields of  $\text{CO}_2$  at varying evaporation temperatures (Figure 3a). At an evaporation temperature of  $50^\circ\text{C}$ , yields of  $\text{CO}_2$  from all *n*-alkane standards  $C_{21}$  and higher were at least 90% of the yield at room temperature. At  $90^\circ\text{C}$ , only yields from  $C_{28}$  and  $C_{30}$  exceeded 90%, whereas yields of shorter homologues were progressively reduced ( $C_{22}$ – $C_{26}$ ) or almost absent ( $<C_{22}$ ). At  $90^\circ\text{C}$ , 80% of  $C_{25}$  *n*-alkane (typically found at the lower end of the higher-plant-wax *n*-alkane range) remained on the wire. At  $100^\circ\text{C}$ , only 60% of  $C_{25}$  *n*-alkane remained. At  $100^\circ\text{C}$ , all *n*-alkane standards  $C_{21}$  and below were at least 90% evaporated and all *n*-alkanes  $C_{26}$  and above were at least 80% retained. The  $\delta$  values for each *n*-alkane standard at each temperature are shown in Figure 3b. There is no systematic isotopic fractionation of any standard as a result of increasing drying-oven temperature and partial volatilization of the sample prior to combustion and measurement. On the basis of these tests, a drying-oven temperature of  $90^\circ\text{C}$  was selected for subsequent investigations.

[16] The sensitivity of the moving-wire system differs from that of irmGCMS only because the split ratio is less favorable. In irmGCMS, the combustion reactor is purged by the chromatographic carrier gas, usually less than  $2.5\text{ mL/min}$ .

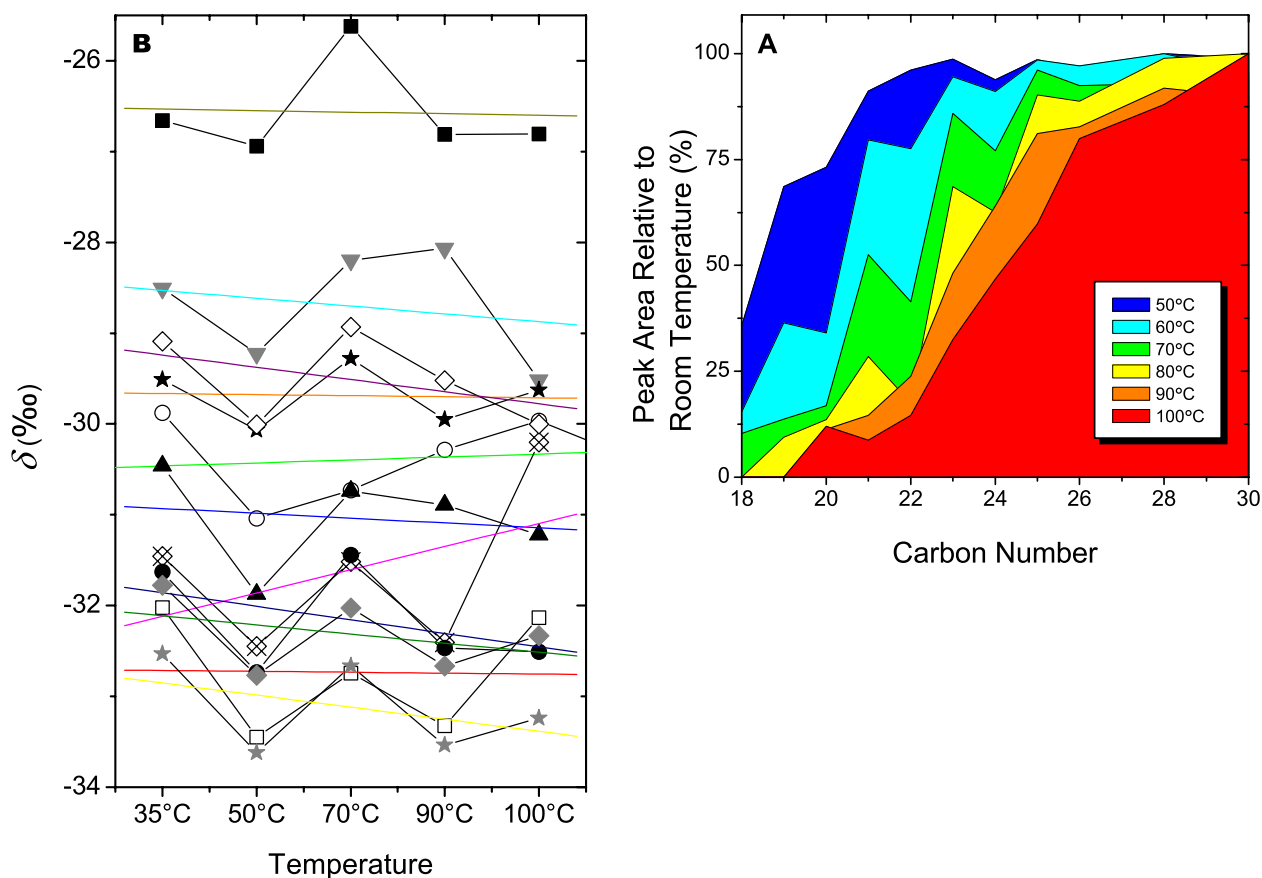


**Figure 3.** Adjustment of operating conditions for the moving-wire system. (a) Retention of *n*-alkanes as a function of carbon number and drying temperatures. For these analyses, the objective was volatilization of the lighter *n*-alkanes. Reported yields are averages of quintuplicate measurements. (b)  $\delta_i$  values of each *n*-alkane standard as a function of drying oven temperature. Linear regression lines are also shown. In no case does the slope differ significantly from zero. C<sub>18</sub>, open squares and red line; C<sub>19</sub>, open circles and green line; C<sub>20</sub>, black triangles and blue line; C<sub>21</sub>, gray inverted triangles and cyan line; C<sub>22</sub>, crossed open diamonds and pink line; C<sub>23</sub>, gray stars and yellow line; C<sub>24</sub>, black circles and dark blue line; C<sub>25</sub>, black stars and orange line; C<sub>26</sub>, open diamonds and purple line; C<sub>28</sub>, black squares and dark yellow line; C<sub>30</sub>, gray diamonds and dark green line.

To prevent intrusion by atmospheric CO<sub>2</sub>, the combustion reactor in the moving-wire system is purged by a flow of 25 mL/min. Accordingly, the fraction of sample carbon transmitted to the mass spectrometer is tenfold to thirtyfold lower. For compound-class analyses, however, there is a compensatory effect. Whereas irmGCMS yields a series of peaks, each of which must be observed separately, compound-class procedures combine all of these into a single peak. The samples used here (100–200 ng C per analysis) are larger than required for irmGCMS but at least tenfold smaller than would be required if an elemental-analyzer system were being used. Moreover, liquid samples can be applied directly to the wire and blank corrections can be based on immediately adjacent baseline signals. In elemental-analyzer systems,

sample cups must be cleaned, loaded, and handled and cup-to-cup variations in the blank are possible.

### 3.2. Test Samples

[17] Extracts from test sediment samples from Great Pond and Mud Patch were used to evaluate the effectiveness of the purification scheme and the accuracy of the resulting isotopic data. Chromatograms of the *n*-alkane fractions after purification, prior to measurement by MW-irMS, are shown in Figures 4a and 4b. The odd-carbon preference typical of plant waxes is evident in both samples. Very small contributions of iso- and anteiso-alkanes are also evident, and an unidentified non-*n*-alkane peak is present between *n*-C<sub>26</sub> and *n*-C<sub>27</sub> in the Mud Patch sample.

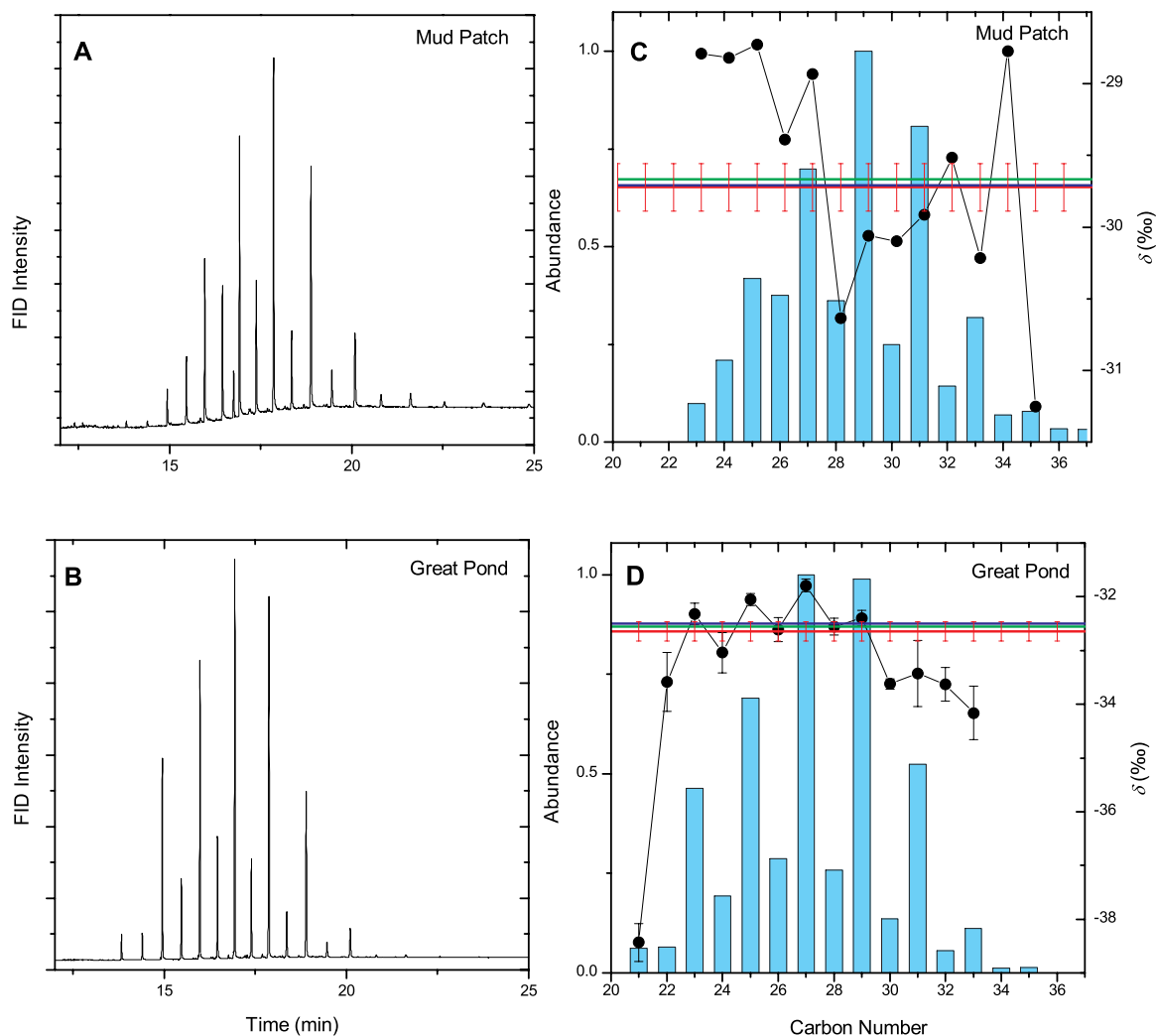


**Figure 4.** Abundances and isotopic compositions of *n*-alkanes in test samples. (a and b) Chromatograms of purified *n*-alkane fractions prior to analysis by MW-irMS. (c and d) Normalized abundances and  $\delta$  values of  $C_{21}$ – $C_{37}$  *n*-alkanes. Also shown are values of  $\delta_{mw}$  (red line, error bars are the s.d. determined from quintuplicate analyses),  $\delta_{w1}$  (green line), and  $\delta_{w2}$  (blue line).

[18] These test samples were also purified using urea adduction [Marlowe *et al.*, 1984] in place of the zeolite/HF treatment. This proved to be less efficient at eliminating branched and cyclic hydrocarbons. In particular, the Mud Patch *n*-alkane sample contained a significant unresolved complex mixture and hence the urea adduction method was not used for subsequent analyses.

[19] Great Pond has a larger contribution of shorter-chain *n*-alkanes, which is evident from the lower average chain length (ACL = 27.99) and maximum contribution from the  $C_{27}$  *n*-alkane. In contrast, ACL for the Mud Patch sample is 28.77 and maximum contribution is from the  $C_{29}$  *n*-alkane. However, both samples contain some shorter chain *n*-alkanes indicative of marine, anthropogenic (e.g.,

fossil fuel), or other nonvascular-plant sources (< $C_{25}$ ). These compounds are partially removed by evaporation during the MW-irMS analysis.

[20] Mud Patch and Great Pond samples were analyzed by MW-irMS at an evaporation temperature of 90°C. Compound-class *n*-alkane  $\delta$  values obtained by MW-irMS ( $\delta_{mw}$ ) are reported in Table 1. For comparison,  $\delta$  values of individual *n*-alkanes were also determined by irmGCMS (Figures 4c and 4d). The expected moving-wire result based on the weighted average of individual *n*-alkanes ( $\delta_{w1}$ ) was calculated as follows:

$$\delta_{w1} = \sum_i X_i \delta_i, \quad (1)$$



where  $X_i$  is fraction of total *n*-alkane abundance and  $\delta_i$  is the individual *n*-alkane  $\delta$  value determined by irmGCMS, with  $i = C_{21} - C_{34}$ , or for the range of *n*-alkanes with individual  $\delta$  values. The difference between the moving-wire result and  $\delta_{w1}$  was 0.05‰ for Mud Patch and 0.08‰ for Great Pond. Neither difference is statistically significant.

[21] Imperfections in the comparison of  $\delta_{mw}$  with  $\delta_{w1}$  could result from partial evaporation of the *n*-alkanes in the intermediate range of carbon numbers ( $C_{22}$ – $C_{28}$ ). If the weighting factors in equation (1) are adjusted to take this into account and the result is denoted by  $\delta_{w2}$  (Table 1) the agreement with  $\delta_{mw}$  is improved for the Mud Patch sample but degraded for the Great Pond sample. In fact, the abundances of the most strongly affected compounds are low enough that the resulting adjustment is smaller than the precision of the measurement.

### 3.3. Case Study: West African Latitudinal Surface Sediment Transect

#### 3.3.1. African Vegetation Belts

[22] The distribution of vegetation on the African continent at present is essentially latitudinal (see Figure 6) [White, 1983]. A large band of tropical rainforest dominated by  $C_3$  vegetation is centered at the equator ( $5^\circ\text{N}$  to  $5^\circ\text{S}$ ).  $C_4$  plants in the rainforest and swamp forest are generally only found along riverbanks and in coastal areas. Further south ( $5^\circ\text{S}$  to  $12^\circ\text{S}$ ), the vegetation shifts to savannah and tropical woodland, where the landscape is defined by a combination of  $C_3$  trees and  $C_4$  grasses. Along the Atlantic coast ( $12^\circ\text{S}$  to  $30^\circ\text{S}$ ) the subtropical grasslands and semideserts are dominated by  $C_4$  grasses. The maximum input from  $C_4$  vegetation to marine sediments comes from the tropical grasslands and semideserts. Prevailing winds (SE trades) during the austral winter, June to August, create a dust plume that travels northeast over the Atlantic at approximately  $15^\circ\text{S}$ . This large dust plume is expected to be the main mechanism for transporting  $C_4$  plant material into marine sediments. The large variation in vegetation belts, and presumably in carbon isotopic compositions, provides a useful test of the sensitivity of compound-class  $\delta$  analysis.

#### 3.3.2. Carbon Number Distributions

[23] The carbon preference index of *n*-alkanes from marine sediments and eolian dusts is generally

lower than that of higher-plant waxes due to inputs of *n*-alkanes from other sources [Simoneit, 1984; Uzaki *et al.*, 1993; Rogers and Savard, 1999]. The CPI for the sediments from the West African Margin was calculated on the basis of the abundance of  $C_{27}$  to  $C_{33}$  *n*-alkanes (see Table 1 for equation). CPI values ranged from 1.29 to 2.69 and are similar to those reported by Huang *et al.* [2000] for marine sediments off N.W. Africa. There are no clear north-south trends in CPI, but the frequently strong odd-carbon preference indicates that plant waxes are an important component of the less volatile *n*-alkanes.

[24] Average chain length was also calculated for all *n*-alkane samples (Table 1). There was no systematic trend in ACL from north to south. Moving southward, the carbon number maximum ( $C_{max}$ ) increases from  $C_{29}$  to  $C_{31}$  but drops to  $C_{27}$  or  $C_{29}$  between  $20.5$  and  $23^\circ\text{S}$ . Similarly, Schefuß *et al.* [2003a] did not observe a trend in ACL as a function of latitude in aerosol samples, but they did observe a shift in  $C_{max}$ . The trend observed in that study was a decrease in  $C_{max}$  from  $30^\circ\text{N}$  to  $10^\circ\text{S}$ . Where these data sets overlap latitudinally, the observed  $C_{max}$  is consistent, as it is with the observations of  $C_{31}/(C_{29} + C_{31})$  by Rommerskirchen *et al.* [2003].

#### 3.3.3. Compound-Class and Compound-Specific Abundances of <sup>13</sup>C

[25] The odd-carbon preferences indicate that plant waxes are present in the sediments from the West African Margin. The carbon-isotopic compositions of the long-chain *n*-alkanes therefore have the potential to carry an environmental signal reflecting the distribution of  $C_3$  and  $C_4$  plants.

[26] Any signal recovered from the sediments must be an imperfect reflection of the actual variations in plant inputs. This is because the alkanes in the sediment derive only in part from plant waxes (if they were pure plant waxes, the carbon-preference indices would be much higher). The compositions of the non-plant-wax components cannot be known precisely, but must include both even-carbon and odd-carbon compounds. For that reason, even analyses which select only the odd-C compounds are bound to reflect mixing of plant-wax, fossil, and marine sources. In favorable cases, that mixing will merely attenuate the plant-related isotopic variations. The observed isotopic variations will be linearly related to the plant-wax signal, but the range of variation will be reduced. This will occur if the nonplant  $\delta$  values and plant/nonplant mixing

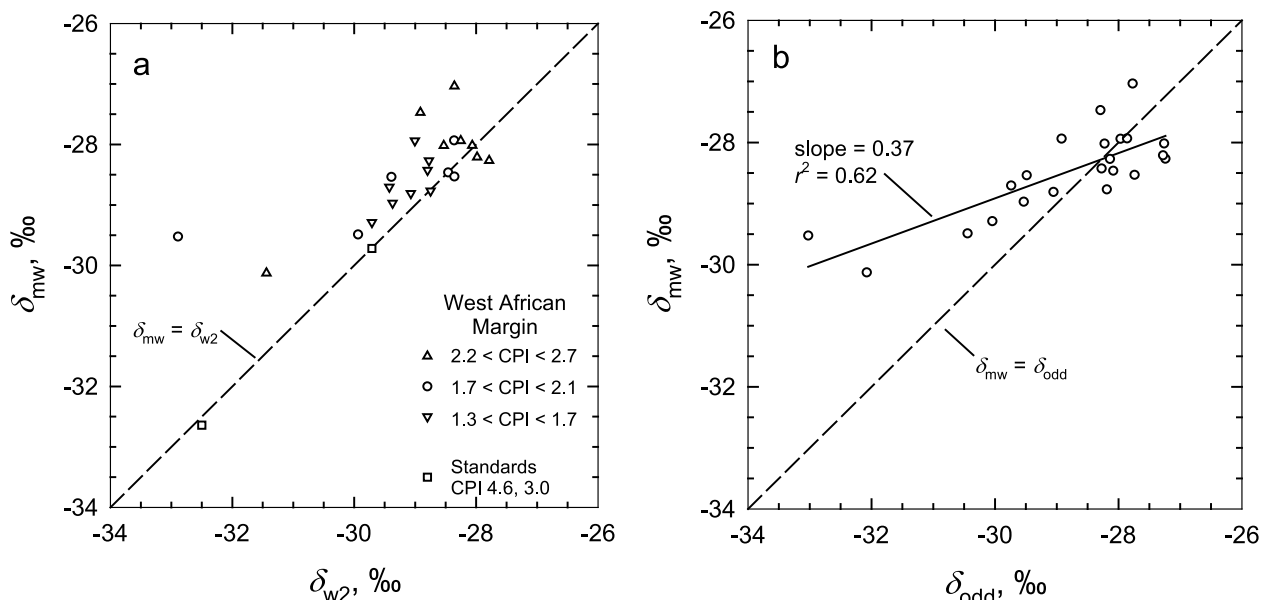


**Figure 5.** (a)  $\delta_{mw}$  versus  $\delta_{w2}$ ; (b)  $\delta_{mw}$  versus  $\delta_{odd}$ .

ratios are uncorrelated with the plant-wax  $\delta$  values. In other cases, the mixing will confound the plant-wax signal, either obscuring or artificially enhancing it. Given only carbon-isotopic and compound-abundance data, the problem is inescapable: all molecules of, for example, an *n*-C<sub>29</sub> alkane have the same structure; it is not possible to separate those from plants from those with other sources (hydrogen-isotopic analyses may eventually allow some resolution of these sources).

[27] The moving-wire analysis includes two additional components: the even-C *n*-alkanes and other materials which may be present but which do not appear in the gas chromatogram. Arguably, inclusion of the even-C homologues is a relatively small step that only extends the mixing effects described. Ideally, the second, non-GC-amenable component would be nonexistent. Solvents were prepared by subboiling distillation to maximize that possibility.

[28] Given these points, it is of interest to examine the isotopic data from the West African transect where marked changes in plant wax  $\delta$  are anticipated [Schefuß *et al.*, 2003b; Rommerskirchen *et al.*, 2003]. Table 1 summarizes the results of compound-specific isotopic analyses, namely values of  $\delta$  for the C<sub>29</sub> *n*-alkane ( $\delta_{29}$ ) as well as the weighted averages  $\delta_{w1}$ ,  $\delta_{w2}$ ,  $\delta_{odd}$  and  $\delta_{even}$  (respectively, the weighted-average  $\delta$  values of the odd- and even-C *n*-alkanes), from irmGCMS. Compound-class *n*-alkane  $\delta$  values obtained by MW-irMS ( $\delta_{mw}$ ) for the same sediments are also

shown. Values of  $\delta_{mw}$  are compared to those of  $\delta_{w2}$  in Figure 5a. This is essentially a test for the presence of non-GC-amenable components. If the sample applied to the moving wire contained only C<sub>21</sub>–C<sub>34</sub> *n*-alkanes, there would be a 1:1 relationship between  $\delta_{mw}$  and  $\delta_{w2}$ . Noise associated with the moving-wire technique could lead to scatter, but the distribution would be centered on the 1:1 line. The moving-wire results instead lie systematically above the 1:1 line and thus indicate that at least one non-GC-amenable component (enriched in <sup>13</sup>C relative to the *n*-alkanes) is present in most of the samples. It may be some material indigenous to the samples which is not a C<sub>21</sub>–C<sub>34</sub> *n*-alkane but which has passed through the sample purification (chromatography, adduction, oxidation). Alternatively, it may represent the hexane-soluble fraction of particulate debris (i.e., dust) that was inadvertently added to the samples in varying amounts during processing (the results are means of tightly grouped quintuplicates, so the scatter cannot represent dust that has fallen onto the moving wire). The absence of any correlation between CPI and  $\delta_{mw} - \delta_{w2}$  ( $r^2 = 0.02$ ,  $n = 22$ ) favors the latter alternative. If so, better precision in future studies may result from sample preparation in a cleaner environment (e.g., use of a laminar-flow hood).

[29] Values of  $\delta_{mw}$  are plotted as a function of  $\delta_{odd}$  in Figure 5b. This is a comparison of the moving-wire result with the otherwise-best-available sediment-based signal. The observed correlation

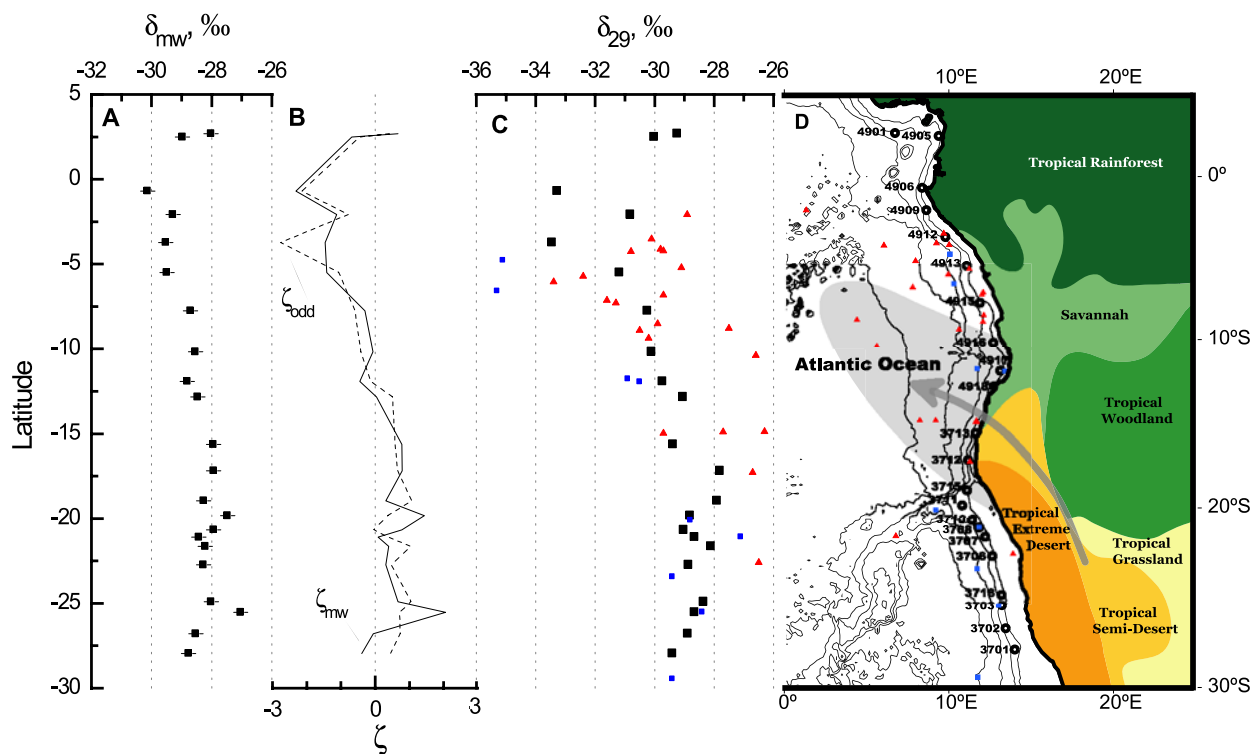


**Figure 6.** (a) Compound-class  $\delta$  values obtained by MW-irMS ( $\delta_{mw}$ ). Points and error bars are means and two standard deviations of the mean for quintuplicate measurements. (b)  $\zeta_{mw}$  and  $\zeta_{odd}$  as defined by equations (2) and (3). (c)  $\delta_{29}$  values. Solid black squares, this study; solid red triangles, Schefuß *et al.* [2003b]; solid blue rectangles, Rommerskirchen *et al.* [2003]. (d) Approximate distribution of vegetation on the African continent. Gray area shows extent of major austral winter dust cloud. Arrow indicates direction of prevailing winds from the interior of the continent. Location (lat., long.) of sediment samples: large open circles, this study; red triangles, Schefuß *et al.* [2003b]; solid rectangles, Rommerskirchen *et al.* [2003].

is highly significant ( $P < 0.01$ ) and provides a basis for examining the utility of  $\delta_{mw}$  as an environmental signal.

### 3.4. Molecular Stratigraphic Potential

[30] Isotopic signals are plotted beside a map of the West African margin in Figure 6. The property most frequently examined by previous investigators is  $\delta_{29}$ , the isotopic composition of the  $C_{29}$  *n*-alkane [Schefuß *et al.*, 2003b; Rommerskirchen *et al.*, 2003]. Values from the present work are plotted along with those from previous studies in Figure 6c. Considerable scatter is evident. Nevertheless, the lowest values of  $\delta_{29}$  coincide with the maximum input of  $C_3$  vegetation from the Congo river drainage basin and higher values, found near 17°S, are consistent with the expected maximum in  $C_4$  inputs due to the prevailing SE trades and the predominance of  $C_4$  vegetation on the adjacent continent.

[31] From an environmental point of view, the key relationship is that between  $\delta_{mw}$  and  $\delta_{odd}$ , the latter being the closest possible approximation of the

plant-wax signal. To examine this, Figure 6b displays values of  $\zeta_{mw}$  and  $\zeta_{odd}$  as a function of latitude. These parameters are defined as follows:

$$\zeta_{mw} = \frac{\delta_{mw} - \overline{\delta_{mw}}}{\sigma_{\delta_{mw}}}, \quad (2)$$

where  $\overline{\delta_{mw}}$  is the mean of the population of values of  $\delta_{mw}$  and  $\sigma_{\delta_{mw}}$  is the standard deviation of that population. Similarly,

$$\zeta_{odd} = \frac{\delta_{odd} - \overline{\delta_{odd}}}{\sigma_{\delta_{odd}}}, \quad (3)$$

where  $\delta_{odd}$  is the weighted-mean isotopic composition of the odd-C *n*-alkanes in a sample and  $\overline{\delta_{odd}}$  and  $\sigma_{\delta_{odd}}$  are the mean and standard deviation of that population, respectively. The transformations represented by equations (2) and (3) have the effect of expressing variations in  $\delta_{mw}$  and  $\delta_{odd}$  on directly comparable scales. As can be seen, the records are roughly congruent. We conclude therefore that  $\delta_{mw}$  is a useful proxy for the isotopic compositions of plant waxes.

[32] Overall, these results demonstrate that a distinct plant wax *n*-alkane  $\delta$  signature can be recovered from aquatic sediments by a combination of sequential chemical purification and analysis by MW-irMS. However, these results also highlight the potential for contamination by non-plant-wax products, both in the sediments and, possibly, during analyses. In future work, it will be important to consider possible contributions from other hydrocarbon sources such as oil seeps or marine inputs and to minimize chances for contamination. Nevertheless, these data and the rate at which the MW-irMS measurements can be obtained make such further investigations worthwhile. If successful, they will pave the way for the use of this compound-class approach for a variety of highly detailed spatial and temporal studies. As well, a basis for using this compound-class approach for the measurement of a variety of other, potentially more exclusive, terrestrial (i.e., *n*-alcohols, fatty acids) and marine (i.e., alkenones, sterols) biomarkers has been established.

#### 4. Conclusion

[33] Analysis of the samples by gas chromatography shows that sequential chemical purification of samples yields a clean *n*-alkane fraction. Removal of most of the shorter chain ( $<C_{25}$ ) *n*-alkanes can be accomplished during the solvent evaporation step of MW-irMS analysis. However, the nonvascular-plant signal cannot be entirely removed, especially when in the same carbon-number range as plant wax *n*-alkanes.

[34] A case study of *n*-alkane  $\delta$  in marine sediments of a latitudinal transect off West Africa yielded results sensitive to the inputs from vegetation on the adjacent continent. The maximum  $C_3$  input was seen off the Congo Basin, where tropical rainforest ( $C_3$  vegetation) is predominant. Maximum  $C_4$  input occurred near  $15^\circ\text{S}$ , where prevailing winds supply maximum  $C_4$  input from the tropical grasslands and semideserts in the far south of Africa. Analysis of the same samples by irmGCMS confirmed these results, providing the basis for the use of this compound class approach for high-resolution, down-core studies.

#### Acknowledgment

[35] We thank Daniel Montluçon for technical support, Carl Johnson for the irmGC-MS analyses, Guillemette Ménot-Combes for help with MW-irMS measurements, and the

WHOI Summer Student Fellow program and NSF (BCS-0218511) for funding.

#### References

- Bird, M. I., P. Giresse, and A. R. Chivas (1994), Effect of forest and savanna vegetation on the carbon-isotope composition of sediments from the Sanaga River, Cameroon, *Limnol. Oceanogr.*, *39*, 1845–1854.
- Brand, W. A., and P. Dobberstein (1996), Isotope ratio-monitoring liquid chromatography mass spectrometry (IRM-LCMS): first results from a moving wire interface system, *Isotopes Environ. Health Stud.*, *32*, 275–283.
- Collister, J. W., G. Rieley, S. Benjamin, G. Eglinton, and B. Fry (1994), Compound-specific  $\delta^{13}\text{C}$  analyses of leaf lipids from plants with differing carbon dioxide metabolisms, *Org. Geochem.*, *21*, 619–627.
- Eglinton, G., and R. J. Hamilton (1963), Leaf epicuticular waxes, *Science*, *156*, 1322–1335.
- Filley, T. R., K. H. Freeman, T. S. Bianchi, M. Baskaran, L. A. Colarusso, and P. G. Hatcher (2001), An isotopic biogeochemical assessment of shifts in organic matter input to Holocene sediments from Mud Lake, Florida, *Org. Geochem.*, *32*, 1153–1167.
- France-Lanord, C., and L. A. Derry (1994),  $\delta^{13}\text{C}$  of organic carbon in the Bengal Fan: Source evolution and transport of  $C_3$  and  $C_4$  plant carbon to marine sediments, *Geochim. Cosmochim. Acta*, *58*, 4809–4814.
- Freeman, K. H., and L. A. Colarusso (2001), Molecular and isotopic records of  $C_4$  grassland expansion in the late Miocene, *Geochim. Cosmochim. Acta*, *65*, 1439–1454.
- Guillet, B., P. Faivre, A. Mariotti, and J. Khobzi (1988), The  $^{14}\text{C}$  dates and  $^{13}\text{C}/^{12}\text{C}$  ratios of soil organic matter as a means of studying the past vegetation in intertropical regions: Examples from Columbia (South America), *Paleogeogr. Paleoclimatol. Paleoecol.*, *65*, 51–58.
- Huang, Y., B. Li, C. Bryant, R. Bol, and G. Eglinton (1999a), Radiocarbon dating of aliphatic hydrocarbons: A new approach for dating passive-fraction carbon in soil horizons, *Soil Sci. Soc. Am. J.*, *63*, 1181–1187.
- Huang, Y., F. A. Street-Perrott, R. A. Perrott, P. Metzger, and G. Eglinton (1999b), Glacial-interglacial environmental changes inferred from the molecular and compound-specific  $\delta^{13}\text{C}$  analyses of sediments from Sacred Lake, Mt. Kenya, *Geochim. Cosmochim. Acta*, *63*, 1383–1404.
- Huang, Y., L. Dupont, M. Sarnthein, J. M. Hayes, and G. Eglinton (2000), Mapping of  $C_4$  plant input from North West Africa into North East Atlantic sediments, *Geochim. Cosmochim. Acta*, *64*, 3505–3513.
- Ikehara, M., K. Kawamura, N. Ohkouchi, M. Murayama, T. Nakamura, and A. Taira (2000), Variations of terrestrial input and marine productivity in the Southern Ocean ( $48^\circ\text{S}$ ) during the last two deglaciations, *Paleoceanography*, *15*, 170–180.
- Kawamura, K. (1995), Land-derived lipid class compounds in the deep-sea sediments and marine aerosols from North Pacific, in *Biogeochemical Processes and Ocean Flux in the Western Pacific*, edited by H. Sakai and Y. Nozaki, pp. 31–51, Terra Sci., Tokyo.
- Krishnamurthy, R. V., and M. DeNiro (1982), Isotopic evidence for Pleistocene climate changes in Kashmir, India, *Nature*, *298*, 640–641.
- Mariotti, A., F. Gadel, P. Giresse, and Kinga-Mouzeo (1991), Carbon isotope composition and geochemistry of particulate organic matter in the Congo River (Central Africa): Application



- tion to the study of Quaternary sediments off the mouth of the river, *Chem. Geol.*, *86*, 345–357.
- Marlowe, I. T., S. C. Brassell, G. Eglinton, and J. C. Green (1984), Long chain unsaturated ketones and esters in living algae and marine sediments, *Org. Geochem.*, *6*, 135–141.
- Meyers, P. A., and R. Ishiwatari (1993), Lacustrine organic geochemistry—An overview of indicators of organic matter sources and diagenesis in lake sediments, *Org. Geochem.*, *20*, 867–900.
- Ohkouchi, N., K. Kawamura, H. Kawahata, and A. Taira (1997), Latitudinal distributions of terrestrial biomarkers in the sediments from the Central Pacific, *Geochim. Cosmochim. Acta*, *61*, 1911–1918.
- O’Leary, M. H. (1981), Carbon isotope fractionation in plants, *Phytochemistry*, *20*, 553–568.
- Rogers, K. M., and M. M. Savard (1999), Detection of petroleum contamination in river sediments from Quebec City region using GC-irMS, *Org. Geochem.*, *30*, 1559–1569.
- Rommerskirchen, F., G. Eglinton, L. Dupont, U. Güntner, C. Wenzel, and J. Rullkötter (2003), A north to south transect of Holocene southeast Atlantic continental margin sediments: Relationship between aerosol transport and compound-specific  $\delta^{13}\text{C}$  land plant biomarker and pollen records, *Geochem. Geophys. Geosyst.*, *4*(12), 1101, doi:10.1029/2003GC000541.
- Schefuß, E., V. Rathmeyer, J. W. Stuut, J. H. F. Jansen, and J. S. Sinninghe Damste (2003a), Carbon isotope analyses of *n*-alkanes in dust from the lower atmosphere over the central eastern Atlantic, *Geochim. Cosmochim. Acta.*, *67*, 1757–1767.
- Schefuß, E., S. Schouten, J. H. F. Jansen, and J. S. Sinninghe Damste (2003b), African vegetation controlled by tropical sea surface temperatures in the mid-Pleistocene period, *Nature*, *422*, 418–421.
- Schulz, H., and Scientific Party (1996), Report and preliminary results of METEOR-Cruise M 34/2, Walvis Bay–Walvis Bay, 29 January–18 February 1996, *Rep. 78*, 133 pp., Geosci. Dept., Univ. of Bremen, Bremen, Germany.
- Schulz, H., and Scientific Party (1998), Report and preliminary results of METEOR-Cruise M 41/2, Malaga–Libreville, 13 February–15 March 1998, *Rep. 114*, 124 pp., Geosci. Dept., Univ. of Bremen, Bremen, Germany.
- Simoneit, B. R. T. (1977), Organic matter in eolian dusts over the Atlantic Ocean, *Mar. Chem.*, *5*, 443–464.
- Simoneit, B. R. T. (1984), Organic matter of the troposphere—III. Characterization and sources of petroleum and pyrogenic residues in aerosols over the western United States, *Atmos. Environ.*, *18*, 51–67.
- Simoneit, B. R. T., R. Chester, and G. Eglinton (1977), Biogenic lipids in particulates from the lower atmosphere of the eastern Atlantic, *Nature*, *267*, 682–685.
- Smith, B. N., and S. Epstein (1971), Two categories of <sup>13</sup>C/<sup>12</sup>C ratios for higher plants, *Plant Physiol.*, *47*, 380–384.
- Uzaki, M., K. Yamada, and R. Ishiwatari (1993), Carbon isotope evidence for oil-pollution in long chain normal alkanes in Tokyo Bay sediments, *Geochem. J.*, *27*, 385–389, 547–574.
- Wagner, T., and L. Dupont (1999), Terrestrial organic matter in marine sediments: Analytical approaches and eolian-marine records of the central Equatorial Atlantic, in *The Use of Proxies in Paleoceanography: Examples From the South Atlantic*, edited by G. Fischer and G. Wefer, pp. 547–574, Springer-Verlag, New York.
- Wagner, T., M. Zabel, L. Dupont, T. Freudenthal, J. Holtvoeth, and C. Schubert (2004), Terrigenous signals in sediments of the low latitude Atlantic—implications to environmental variations during the late Quaternary: Part I: Organic carbon, in *The South Atlantic in the Late Quaternary: Reconstruction of Material Budget and Current Systems*, edited by G. Wefer, S. Mulitza, and V. Rathmeyer, pp. 295–322, Springer-Verlag, New York.
- Westerhausen, L., J. Pnynter, G. Eglinton, H. Erlenkeuser, and M. Sarnthein (1992), Marine and terrigenous origin of organic matter in modern sediments of the equatorial east Atlantic: The  $\delta^{13}\text{C}$  and molecular record, *Deep Sea Res., Part A*, *40*, 1087–1121.
- White, F. (1983), *The Vegetation of Africa: A Descriptive Memoir to Accompany the UNESCO/AETFAT/UNSO Vegetation Map of Africa*, 356 pp., UNESCO, Paris.
- Zhao, M., L. Dupont, G. Eglinton, and M. Teece (2003), *n*-Alkane and pollen reconstruction of terrestrial climate and vegetation for N.W. Africa over the last 160 kyr, *Org. Geochem.*, *34*, 131–143.